

Apparent vibrational side bands in π -conjugated systems: The case of distyrylbenzene

C. C. Wu,¹ E. Ehrenfreund,^{1,2} J. J. Gutierrez,³ J. P. Ferraris,³ and Z. V. Vardeny¹

¹Department of Physics, University of Utah, Salt Lake City, Utah 84112, USA

²Department of Physics and Solid State Institute, Technion-Israel Institute of Technology, Haifa 32000, Israel

³Nano Tech Institute, University of Texas at Dallas, Richardson, Texas 75083, USA

(Received 14 October 2004; revised manuscript received 28 December 2004; published 2 February 2005)

The photoluminescence (PL) spectra of dilute solution and single crystals of distyrylbenzene show unique temperature-dependent vibronic structures. The characteristic single frequency progression at high temperatures is modulated by a low-frequency progression series at low temperatures. None of the series side-band modes corresponds to any of the distyrylbenzene Raman frequencies. We explain these PL properties using a time-dependent model with temperature-dependent damping, in which the many-mode system is effectively transformed to two “apparent” modes and then to a single apparent mode as damping increases.

DOI: 10.1103/PhysRevB.71.081201

PACS number(s): 78.55.Kz, 71.55.Ht, 78.30.Jw, 78.66.Qn

The excited state properties of distyrylbenzene (DSB), which is the three-phenyl group oligomer analog of *p*-phenylene vinylene (Fig. 1, inset), have been the subject of recent experimental^{1,2} and theoretical³ spectroscopic studies, because of potential optoelectronic applications.⁴ DSB-photoluminescence (PL) spectroscopy has been the subject of numerous research studies, since it is strongly dependent upon the packing order.^{3,5–7} In DSB films the molecules form H aggregates, thus substantially weakening the emission quantum yield, relative to the separate oligomers in dilute solutions.⁵ This is especially true in DSB single crystals: due to the herringbone symmetry, the fundamental optical transition (the so-called 0-0 transition) is either totally absent or significantly reduced.^{3,5} Typical PL spectra of DSB chromophores contain vibronic progression series, of which the relative intensity and frequencies depend on packing and temperature. One key feature of the vibronic progression is that the side-band replicas have apparent frequencies that do not match *any* of the Raman active modes. This is true also for many other π -conjugated polymers and oligomers: the rich Raman spectrum of the multivibrational modes systems is reduced to only one, or two apparent vibronic progression in their PL spectrum.

In this paper, we account for the apparent modes that appear in the PL spectra of DSB dilute solutions and single crystals; the same model may be used to explain the PL spectra of other π -conjugated systems. We use the preresonance Raman spectrum in order to quantify the relative configuration displacement [or, equivalently, the Huang-Rhys (HR) factor] for each of the vibrational modes. Consequently, we utilize the relative HR factors in a damped time-dependent model to calculate the DSB-PL spectrum. We found that above a certain finite damping, the PL vibronic progression contains only a single apparent vibronic frequency. For lower damping, however, the single-frequency progression is modulated by a low-frequency progression, in excellent agreement with the PL spectra measured at low temperatures.

In Fig. 1(a) we show the PL spectra of DSB in dilute frozen solution of tetradecane⁶ at low and high temperatures. The PL spectrum at 200 K has the typical vibronic progression shape of other π -conjugated systems, but

notable changes occur with decreasing temperature. At 200 K [Fig. 1(a), bottom curve], there appears a dominant high-frequency vibronic progression of $\hbar\omega_H \approx 0.17$ eV (≈ 1370 cm⁻¹), which, however, does not match any of the Raman modes (Fig. 2), and is not even in the vicinity of highly coupled modes (Table I). The highest energy peak (marked “0”) is the fundamental optical transition ($1A_g \rightarrow 1B_u$, at 3.15 eV), whereas the lower energy peaks (marked “1,2,3”) are the higher-order vibronic side bands. As the temperature is lowered, however, the high-frequency progression is modulated [Fig. 1(a), 20 K] by a different low-frequency progression of $\hbar\omega_L \approx 17$ –19 meV. We denote this modulated vibronic structure by k,n ($k=0,1,2,3$, $n=0,1,2,\dots$), where k (n) is the order of the high- (low-) frequency modulation. The appearance of these vibronic replicas is further illustrated in Fig. 1(b), where we show the PL Fourier transform, namely, $|\int PL(E) \exp(-iEt/\hbar) dE|$. At 200 K, only highly damped short-period (≈ 0.02 ps) oscillations are observed. At 20 K, on the contrary, there is considerably less damping and the short-period oscillations pattern is modulated by a long-period (≈ 0.22 ps) component.

The PL spectra of DSB single crystal at 4 and 200 K are shown in Fig. 1(c). The overall vibronic structure is very similar to that of the solution: a single-frequency vibronic progression at 200 K is modulated by a much lower frequency at 4 K. The main difference between the solution and single crystal PL spectra is the intensity of the fundamental (0) transition: in DSB crystals it is unobservable at 200 K, gradually increasing as the temperature is lowered,⁷ reaching approximately $\approx 15\%$ of its solution relative strength at 4 K. The suppressed strength of the 0 transition is the result of the crystal symmetry.³

When trying to account for the PL emission spectrum of a multivibrational system, such as DSB, in relation with its Raman spectrum, it is useful to employ time-dependent analysis rather than the often used sum-over-states Franck-Condon approach.⁸ In general, the emission spectrum $F(E)$ (E is the photon energy) is given⁹ by the Fourier transform of the time-dependent autocorrelation function of the transition dipole moment, $f(t)$,

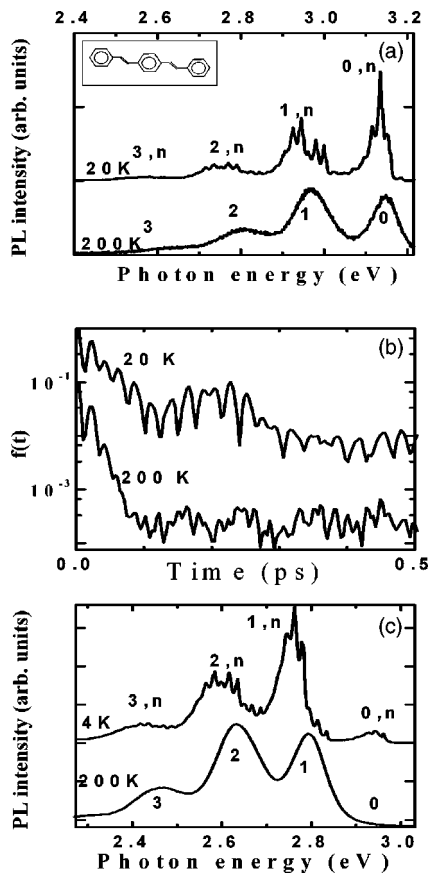


FIG. 1. PL spectroscopy of DSB. (a) Solution spectra at 20 and 200 K. The indices 0 and 1,2,3 in the 200 K spectrum denote the fundamental and vibronic replica transitions, respectively. The pairs of indices k,n ($k=0,1,2,3$) in the 20 K spectrum denote the complex modulated vibronic structure (see text). Inset: The chemical structure of DSB. (b) The Fourier transform of the PL spectra shown in (a). Note the fast decrease at 200 K and the long-period modulation at 20 K. The 200 K curve is vertically displaced for clarity. (c) The same as in (a) but for a DSB single crystal. Note the missing fundamental transition at 200 K and its finite, but small, intensity at 4 K.

$$F(E) = \int_{-\infty}^{\infty} f(t) e^{iEt/\hbar} dt. \quad (1)$$

Following Ref. 9, we write the correlation function for a multimode system in the harmonic approximation and linear electron-phonon coupling as

$$f(t) = |P|^2 e^{-iE_0 t/\hbar - S_+(t) + S_-(t)} e^{-\Gamma|t|},$$

$$S_{\pm}(t) = \sum_j S_j w_j^{\pm} e^{\mp i\omega_j t}, \quad S = \sum_j S_j (2n_j + 1), \quad (2)$$

where P is the dipole matrix element for the relevant optical transition and E_0 is the bare optical transition energy. In Eq. (2), j is the mode index, $w_j^+ = w_j^- + 1 = n_j + 1$, where $n_j = 1/[\exp(\hbar\omega_j/k_B T) - 1]$ is the mode occupation number at temperature T , $S_j = \omega_j \Delta_j^2 / 2\hbar$, and Δ_j is its equilibrium (normal coordinate) displacement in the optically excited electronic state relative to the ground state. We emphasize here

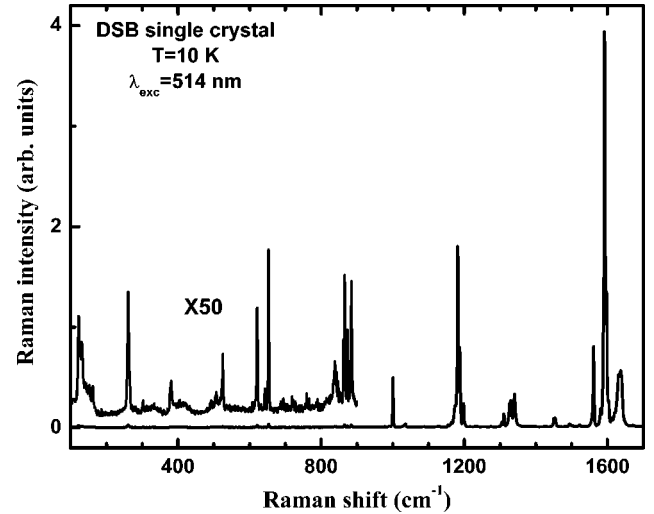


FIG. 2. Raman spectrum of a DSB single crystal at preresonant conditions.

that it is the “electron temperature,” T_e , which determines the mode occupation, n_j . T_e is determined by the photon excitation energy and the electron excess energy relaxation rate and may be considerably higher than the lattice temperature, T . We identify S with the system HR factor, which is the sum of the individual HR factors modified by the temperature [Eq. (2)]. The time-dependent term $S_+(t)$ in Eq. (2) is responsible for the redshifted vibronic side bands in the PL spectrum, while $S_-(t)$ gives rise to blueshifted side bands, emphasizing the low-frequency modes at relatively high T_e . In Eq. (2), a simple mode-independent phenomenological damping, $\Gamma \geq 0$, is introduced; it represents losses due to the natural line broadening and/or other degrees of freedom.⁸ Note that $f(t)$ in Eq. (2) is a product of various periodical functions, $\exp(-i\omega_j t)$, each with a different period and amplitude. Thus, the effect of finite damping is to limit the effective time domain in the integral [Eq. (1)], emphasizing partial periodic recurrences in $f(t)$ that result in apparent vibronic frequencies in the PL spectrum. The apparent mode (APM) frequencies need not be equal to one of the observed Raman modes, but are related to them in a nontrivial way.¹⁰ An example of

TABLE I. The most intense Raman lines of crystalline DSB at 10 K. ν_j , I_j/I_{10} and S_j/S , respectively, denote the measured peak frequency, relative integrated intensity and the calculated relative HR factor [Eq. (3)], for each mode.

j	1	2	3	4	5	6
$\nu_j(\text{cm}^{-1})$	131	261	640	873	1000	1181
$I_j/I_{10}(\%)$	1.16	0.45	0.71	0.77	6.7	50
S_j/S	0.35	0.039	0.01	0.01	0.035	0.19
j	7	8	9	10	11	
$\nu_j(\text{cm}^{-1})$	1330	1452	1561	1591	1635	
$I_j/I_{10}(\%)$	19	2.7	13	100	42	
S_j/S	0.058	0.007	0.027	0.20	0.078	

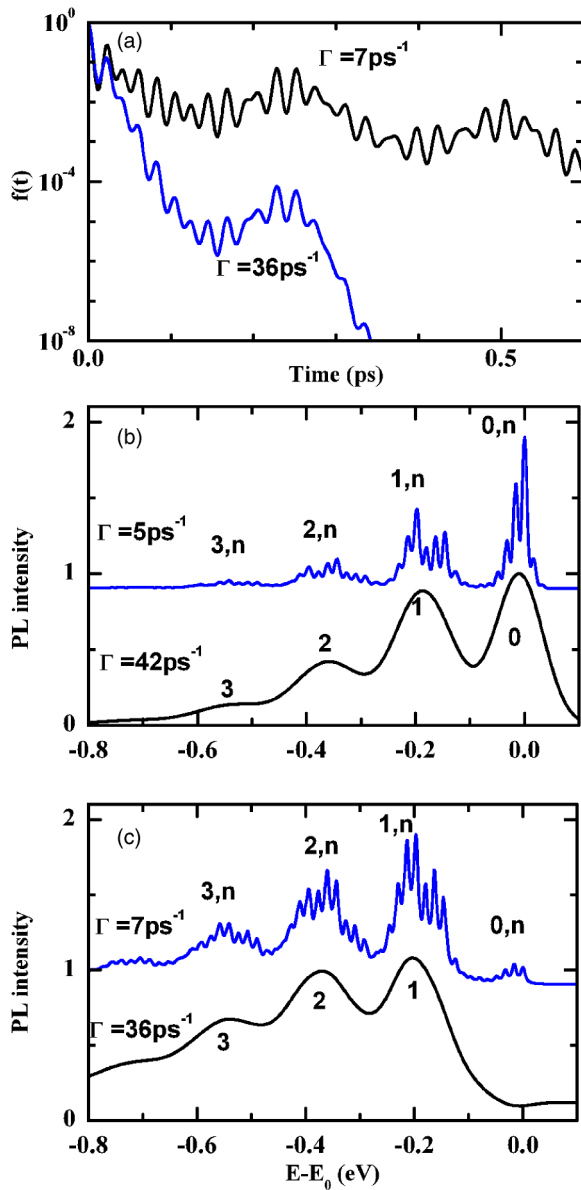


FIG. 3. Model calculations of DSB PL spectra using the 11-mode system of Table I for Γ as shown. (a) The normalized dipole autocorrelation function $f(t)$ [Eq. (2)] for $S(0)=2.5$, $T_e=4$ (200) K for the upper (lower) curve; note the logarithmic scale. (b) The PL spectra obtained by the Fourier transform of $f(t)$ similar to that in (a), but for $S(0)=1.7$, $T_e=150$ (200) K for the upper (lower) curve. E_0 is the energy of the fundamental transition. (c) The PL spectra obtained by the Fourier transform of $f(t)$ for the parameters as in (a), but for the totally suppressed (bottom) and 85% suppressed (top) fundamental transition.

this effect is shown in Fig. 3(a), where $f(t)$, calculated using the 11-mode system of DSB given in Table I, is plotted on a logarithmic scale. It is clearly seen, that even for low damping [Fig. 3(a), top], $f(t)$ is dominated by two APMs: a high-frequency (short-period) APM_H , modulated by a low-frequency (long-period) APM_L . The main effect of the damping is the faster decrease of the low-frequency component [Fig. 3(a), bottom].

The HR factors that determine the vibronic structure are

closely related to the measured Raman spectrum, since the Raman process is enabled by the electron-phonon interaction. The $T=0$ intensity (I_j^0) of each Raman line measures its excited state displacement:⁸ $I_j^0 \propto \omega_j^3 \Delta_j^2$. We then have⁹ $S_j \equiv \omega_j \Delta_j^2 / 2\hbar \propto I_j^0 / \omega_j^2$ and,

$$S_j/S(0) = \left[\sum_{j'} (I_{j'}/I_j^0) (\omega_j/\omega_{j'})^2 \right]^{-1}, \quad (3)$$

where $S(0)$ is S at $T=0$ K. We note that the ω_j^{-2} factor in S_j emphasizes the lower frequency Raman modes in the PL spectrum. This can be seen in Table I, where we list for DSB $S_j/S(0)$, calculated using Eq. (3) and the Raman data (Fig. 2): the lowest frequency mode has the largest HR factor, although its intensity is $\approx 1\%$ of the strongest line. We conclude then: (1) The apparent modes are the result of a weighted beating of all Raman frequencies. (2) The frequencies of the apparent modes are not, in general, the simple sum or difference of the Raman frequencies, and cannot therefore be predicted *a priori*. (3) The relative intensities of the apparent vibronic structure of the PL spectrum is solely determined by the experimentally measured preresonant Raman spectrum. (4) The only fitting parameters needed are the overall damping and the absolute magnitude of the total HR factor.

The first excited state of isolated DSB molecules is optically allowed, making them strongly luminescent and usable as the active media in light-emitting devices.⁴ Typically, the PL spectrum of isolated DSB molecules consists of the fundamental (0-0) optical transition and a single-frequency phonon sidebands replica series. However, in DSB and other *p*-oligophenylene vinylenes, as well as oligothiophenes,² in the form of solid films and crystals, the 0-0 band is strongly suppressed, whereas the phonon replicas retain their intensity and dominate the PL spectrum.^{5,11} The 0-0 PL band in films and crystals is forbidden due to Davydov splitting associated with H aggregates. The 0-0 intensity depends on the film morphology (or aggregate size) and/or crystal purity. In an inhomogeneous solid sample, the resulting emission spectrum may be composed of contributions from several domains, with various 0-0 to 0- n intensity ratio. We therefore discuss separately the emission spectra of solution and crystalline DSB.

Using the data of Table I we show in Fig. 3(a) the dipole autocorrelation function, $f(t)$, generated for low and high damping. It is visually striking that the 11-mode system is dominated by only two APM: a short-period mode modulated by a long-period mode. Moreover, the frequency associated with these two APMs does not coincide with any DSB normal mode. The data given in Table I are also used to generate the PL spectra shown in Fig. 3(b). Here the values of the electron temperature, T_e , HR factor S and damping Γ were chosen to best fit the frozen solution experimental data at low and high lattice temperatures, T [Fig. 1(a)]. The higher damping spectrum that presumably occurs at $T=200$ K [$\Gamma=42$ ps⁻¹, Fig. 3(b)] shows a vibronic progression dominated by a single frequency, $APM_H=173$ meV (≈ 1400 cm⁻¹). These progression peaks are marked as "1,2,3." This is in excellent agreement with the data at 200 K

[Fig. 1(a), bottom curve]. For this case we chose $T_e = T$, since the relevant modes are at high frequencies. At lower lattice temperatures we expect the damping to decrease. Consequently, the low-frequency APM is less suppressed, making the PL spectrum sensitive to the actual value of T_e . At low Γ values, there appears a low-frequency modulation (with $\text{APM}_L \approx 17$ meV) of the high-frequency vibronic series, as seen in Fig. 3(b) (top curve). The combined progression peaks are denoted as (k, n) , where $k=0,1,2,3$ denotes the APM_H progression and $n=0,1,2,\dots$ denotes the APM_L modulation of APM_H . The PL spectrum in Fig. 3(b) (top curve) was calculated using $T_e=150$ K; it shows two blueshifted peaks, in very good agreement with the experimental data at $T=20$ K [Fig. 1(a), top curve]. We thus conclude that due to the nonresonant PL excitation, $T_e > T$.

The crystalline PL spectra show similar characteristics to the Solution spectra; i.e., at high temperatures it is dominated by a single APM, whereas at low temperatures this structure is modulated by a low-frequency APM. As for the solution spectra, this behavior naturally results from a decreased damping at low temperatures. However, the crystalline spectra reveal an additional feature not observed in solutions.

It is seen in the PL spectra of crystalline DSB [Fig. 1(c)], that the band centered at ≈ 2.95 eV appears at $T=4$ K but not at $T=200$ K. Measurements at intermediate temperatures⁷ reveal that its intensity monotonically decreases with increasing temperature; above $T=150$ K it cannot be observed any longer. We interpret this band as the fundamental optical transition that is suppressed by the crystal symmetry. However, the vibronic structure below ≈ 2.95 eV is not affected.³ In order to quantitatively account for the temperature-dependent crystalline PL spectra, we have allowed the 0 transition to vary independently of all other phonon-mediated transitions.

First, we recognize that the $S_+(t)$ terms in Eq. (2) are responsible for all the redshifted spectral features associated with the electron-phonon interaction. The time-independent term S in Eq. (2) gives the intensity of the fundamental optical transition in the presence of the coupled vibrational modes. Second, assuming that the fundamental optical transition has a small finite width of $\hbar\Gamma_0$, we calculate its inten-

sity [denoted $I_0(E)$] using Eq. (2) while taking into account only those modes whose frequency is smaller than Γ_0^{-1} . We then let I_0 be partially suppressed, and write for the crystalline PL spectrum,

$$F_{\text{cryst}}(E) = F(E) - \alpha I_0(E), \quad (4)$$

where $F(E)$ is given by Eq. (1), and α is the suppression parameter controlling I_0 in the crystalline spectrum. Using Eq. (4), the data of Table I, and $\hbar\Gamma_0=4$ meV we show in Fig. 3(c) a high-temperature (200 K, $\Gamma=36$ ps⁻¹) PL spectrum with totally suppressed fundamental transition, namely $\alpha=1$. This is in excellent agreement with the $T=200$ K crystalline spectrum [Fig. 1(c)].

Allowing now for a nonzero I_0 intensity ($\alpha < 1$) together with a smaller Γ , we can account for the finite intensity fundamental transition and the low-frequency modulation of the high-frequency APM observed in crystalline PL spectra at low temperatures. An illustrative example is shown in Fig. 3(c) for the $T=4$ K spectrum, where I_0 is 85% suppressed and $\text{APM}_L \approx 17$ meV; again, in very good agreement with the 4 K crystalline spectrum [Fig. 1(c)].

In summary, we showed that the apparent low-frequency vibronic side band in the crystalline PL spectrum is inherent to the DSB chromophore; it is not related to the strength of I_0 , as previously suggested for oligothiophene crystals.² We interpret the blueshifted small peaks above the 0-0 transition, in the frozen solution spectrum, as due to “hot luminescence.” Using a time-dependent model with temperature-dependent damping, we showed that the many-mode DSB system is effectively transformed into two apparent modes then to a single apparent mode as damping increases. In general, increased damping in multivibrational-mode π -conjugated systems results in effective elimination of vibrational modes from the emission and absorption spectra and the eventual appearance of a nearly regularly spaced progression at an apparent frequency. Knowing the Raman spectrum, it is possible then to account in detail for the emission and absorption spectra of π -conjugated systems.

Supported by DOE Contract No. FG-02-04 ER46109 and Israel Science Foundation Grant No. 735/04.

¹I. Orion, J.P. Buisson, S. Lefrant, *Phys. Rev. B* **57**, 7050 (1998).

²F. Meinardi, M. Cerminara, S. Blumstengel, A. Sassella, A. Borghesi, and R. Tubino, *Phys. Rev. B* **67**, 184205 (2003).

³F.C. Spano, *J. Chem. Phys.* **114**, 5376 (2001); **116**, 5877 (2002); **118**, 981 (2003); **120**, 7643 (2004).

⁴G. Hadziioannou, in *Semiconducting Polymers: Chemistry, Physics, and Engineering*, edited by G. Hadziioannou and P. F. van Hutten (Wiley, New York, 2000), Chap. 7.

⁵D. Oelkrug, H.-J. Egelhaaf, J. Gierschner, and A. Tompert, *Synth. Met.* **76**, 249 (1996); D. Oelkrug, A. Tompert, J. Gierschner, H.-J. Egelhaaf, M. Hanack, M. Honloch, and E. Steinhuber, *J. Phys. Chem. B* **102**, 1902 (1998); H.-J. Egelhaaf, J. Gierschner, and D. Oelkrug, *Synth. Met.* **83**, 221 (1996); J. Gierschner, H.-J. Egelhaaf, and D. Oelkrug, *ibid.* **84**, 529 (1997).

⁶J. Gierschner, H.-G. Mack, L. Lüer, and D. Oelkrug, *J. Chem. Phys.* **116**, 8596 (2002).

⁷C. C. Wu, M. C. Delong, Z. V. Vardeny, J. J. Gutierrez, and J. P. Ferraris, *Synth. Met.* **137**, 939 (2003).

⁸E.J. Heller, R.L. Sundberg, and D. Tannor, *J. Phys. Chem.* **86**, 1822 (1982).

⁹S. Nakajima, Y. Toyozawa, and R. Abe, in *The Physics of Elementary Excitations*, edited by P. Fulde, Springer Series in Solid State Sciences Vol. 12 (Springer-Verlag, Berlin, 1980).

¹⁰Similar conclusions (limited though to $T=0$ K) were reached by L. Tutt, D. Tannor, J. Schindler, E. J. Heller, and J. I. Zink, *J. Chem. Phys.* **87**, 3017 (1983).

¹¹P. A. Lane, H. Mellor, S. J. Martin, T. W. Hagler, A. Bleyer, and D. D. C. Bradley, *Chem. Phys.* **257**, 41 (2000).